Zinc salt Mediated Synthesis, Growth kinetic and Shaped Evolution of Silver Nanoparticles

Dare, E. O.* [1,2,3,5], Makinde, O.W. [2], Ogundele, K.T. [2], Osinkolu, G.A. [2], Fasasi, Y.A.[2], Sonde, I.[1] Bamgbose, J.T[1]., Maaza, M. [3], Sithole, J.[3] Ezema, F.[4], Adewoye, O.O.[5]

[1] Department of Chemistry, University of Agriculture, Abeokuta, Nigeria

[2] Center for Energy Research and Development, Obafemi Awolowo University, Ile-Ife, Nigeria

[3] Nanosciences Laboratories, Materials Research Department, iThemba LABS, Somerset West, South Africa.

[4] Department of Physics, University of Nigeria, Nssuka, Nigeria

[5] National Agency for Science and Engineering Infrastructure, Idu Industrial Area, Abuja, Nigeria

*Corresponding author: dare3160@hotmail.com

Abstract: We report the synthesis of various shaped silver nanoparticles mediated by $ZnCl_2$ salt. It has been demonstrated that the salt, $PVP/AgNO_3$ mole ratio and the type of polyol (EG, DEG, GL) significantly determined twinning probability which is an index of silver seed growth origin. High twining probability arising from low PVP/Ag^+ ratio and 50 mole% salt favours 1D grown nanowires and nanorods whereas low twinned amidst high mole% salt (150) in DEG offered 2D grown nanoflakes and nanosheets. Other shaped silver nanoparticles have been found. Accidentally, we arrived at a core – shell heterostructure of Ag–ZnO nanocomposite with Ag core enrichment when mole% of the salt was made up to 300. Growth kinetic of nanosphere obtained was monitored and effect of salt mediation was found crucial. Structural evolution of shaped Ag nanoparticles and the nanocomposite have been monitored using XRD, SEM, EDX, TEM and UV/vis.

Keywords: shaped silver nanoparticles; growth kinetic; zinc salt; polyol

Introduction

Nanostructured materials have received broad attention due to their distinguished performance in electronic, optic and photonics [1]. With reduction in size, novel electrical, mechanical, chemical and optical properties are introduced which are largely believed to be the result of surface and quantum confinement effects. They have been widely exploited for use in photography, catalysis, biological labeling, photonic, optoelectronic, information storage and formulation of magnetic ferrofluids [2-4].

Among the various metal nanostructures, silver nanoparticles (SN) have been widely investigated because they exhibit unprecedented optical, electronic and chemical properties, depending on their sizes and shapes, thus opening many possibilities for diverse technological applications [5-7].

Generally, silver nanoparticles have been produced by various methods including chemical reduction of silver ions with or without [8,9] stabilizing agents, thermal decomposition of organic solvents and electrospining [10]. Using these methods [8-14], silver nanoparticles with spherical, octahedral, tetrahedral, hexagonal, cubic, wire, coaxial cable, triangular prism, disc and belt shapes have been produced. Apart from metal – silver nanobimetallics [15-19], functionalization or core – shell of silver–metal oxide nanocomposites are limited in the literature. Ag–ZnO electrical contact material was only recently produced using mechanochemical synthesis route [21]. Polymer functionalized silver has been reported [22]. Furthermore, the presence of various ions has been shown to influence the shape and size of metallic nanostructures produced via the polyol method. Xia group [23] has shown that the presence of iron (II) or iron (III) in the polyol synthesis facilitates the growth of silver nanowires or cubes, depending on the concentration of iron ions. Copper salts [24] have been used to effect polyol reduction of silver nitrate.

In this present paper, we report the synthesis of various shaped silver nanoparticles and for the first time zinc oxide – wrapped silver (core – shell) nanocomposite using chemical reduction in a polyol process under the influence of zinc chloride salt. Shapes of the silver and silver core–zinc oxide shell nanoparticles have been followed by various techniques such as XRD, TEM, EDX and UV – vis spectroscopy.

Experimental

Materials

The experiments were conducted using analytical grade Zinc chloride ($ZnCl_2$) Silver nitrate ($AgNO_3$), Polyvinylpyrrolidone (PVP) powder (PVP, lot analysis, 96.2%, MW = 1,300000). All solvents [ethylene glycol (EG), diethylene glycol (DEG) and, glycerol (GL)] were used without purification. All chemicals and solvents were commercially obtained from Sigma – Aldrich Chemicals.

Characterization

X-ray diffraction (XRD) measurements were performed on D8 Advanced Bruker X – ray diffractometer, with Cu Kα1 radiation (λ = 0.154060 nm at 40 KV and 40 mA). Scanning electron microscope (SEM) images were

recorded on a field emission scanning electron microscopy (FESEM, Quanta 200F, HV 15.0 kV) coupled with an energy – dispersive X – ray spectrometer (EDX, Genesis 2000). Transmission electron microscope was carried out using Model 3010 JEOL microscope operating at 300 kV. The uv – visible spectra were measured with a Shimadzu UV – 2450 spectrometer.

Synthesis

Shaped silver nanoparticles

The shaped silver nanoparticles were synthesized by chemical reduction method in a polyol process. The polyols used which served as the reducing agents were ethylene glycol (EG), diethylene glycol (DEG) or glycerol (GL). Molar concentrations of reactants were prepared in the probe solvent unless otherwise stated. PVP served as protective stabilizing agent while zinc chloride (salt) is expected to facilitate reduction process and seed formation. The molar ratio PVP/Ag^+ was set within the range 0.3 – 2.0. 10% - 300% mole of the salt (relative to silver nitrate) was used unless otherwise stated.

In a typical procedure, 20 mL of the polyol [EG, DEG, TEG, GL] was heated to 100 ^{o}C with stirring for 30 min. A solution containing 5.0 mM silver nitrate and 0.5 mM (10%) were added to the stirring polyol [EG, DEG, TEG or GL]. Polyol solution of PVP (2.5 mM) was injected over a period of 5 min and thereafter temperature of 180 ^{o}C was maintained. Reflux condition was used for the core-shell synthesis. The colloidal system was cooled to room temperature and silver nanoparticles separated from the liquid by centrifugation and then washed with acetone and ethanol.

Results and discussion

Growth and nucleation of SN was apparently noticed as PVP was introduced. The reactant mixture changes quickly from colorless to yellow after the addition of PVP and $ZnCl_2$ salt solution in EG. Yellow to light greenish opaque colloidal color transition which was maintained for more than 40 minutes served to indicate a complete reaction. Turbid brown, wispy gray and wispy gray colors were the final colour marking a complete reaction in the case when reducing solvent was GL, DEG and TEG respectively. The colour changes in nanomaterial synthesis are due to confinement of electrons and consequent changes in electronic energy levels [9].

The XRD pattern of a typical silver nanoparticle synthesized in this study are almost identical regardless of experimental condition (Figure 1b) and which is a reflection of high degree of crystallinity.
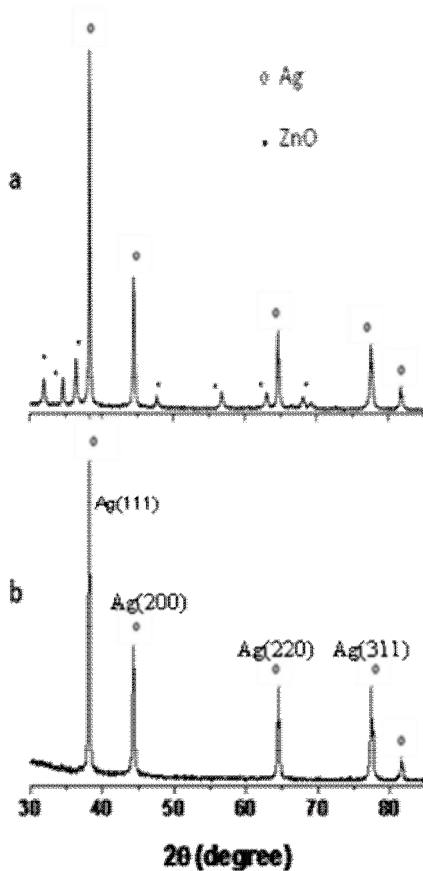
Figure 1: XRD pattern of as – prepared (a) Silver core–ZnO shell nanocomposite (b) silver sample

This indicates that all of the diffraction peaks can be readily indexed to face – centered cubic (fcc) silver with a calculated lattice constant of 4.1 Å.

Effects of Polyols, PVP/Silver nitrate mole ratio and Salt

It has been established that morphology, sizes and size distribution of metallic nanoparticles depends on some reaction conditions such as temperature, time, concentration, PVP/Ag$^+$ mole ratio and style of reagents addition [8] as it affects whether nucleation is homogeneous or heterogeneous [25]. The synthesis conditions used for producing the various shaped SNs are summarized in table 1.

Table 1. Synthesis conditions for various shaped silver nanoparticles

| Sample	PVP:AgNO$_3$ (mole ratio)	ZnCl$_2$ (mole %)	Temperature (^{o}C)	Time (min)	Mean Size	Polyol	Shape and figure ID (2a-l)
1	0.5	10	180	75	48 nm	EG	Nanosphere (c)
2	1.0	50	180	75	5 – 30 μm (Length) 20 – 26 nm (diameter)	EG	Nanowire (h)
3	0.3	50	180	75	20 – 50 μm (length) 33 – 42 nm (diameter)	EG	Nanowire (i)
4	0.5	30	180	90	Not determined	DEG	Nanowire and nanoparticles (g)
5	1.0	150	180	90	82 – 131 nm (thickness)	DEG	Nanoflakes (e)
6	2.0	150	180	90	60 – 110 nm (thickness)	DEG	Nanosheet (f)
7	1.0	100	180	180	Not determined	GL	Fluffy nanocake (k)
8	0.5	0	180	120	75 – 81 nm	EG	Quazi nanosphere (d)
9	1.0	0	180	120	41 nm	EG	Multiply twinned (a & b)
10	2.0	0	180	120	78 - 83 nm (diameter) 354 – 401 nm (length)	EG	Nanorod (j)
11	1.0	300	reflux	90	110 nm	EG	Agglomerated Ag /ZnO nanocomposite (l)

Apparently, nature of the polyol, PVP/silver nitrate ratio and fraction of the salt added affected shapes, sizes and reaction time significantly. The reaction in the presence of EG where PVP/Ag mole ratio (0.5) and 50 mole% ZnCl$_2$ salt

were adopted produced nanowires whose length and diameter are in the range 5 – 30 µm and 20 – 26 nm respectively (table 1, Fig. 2h).
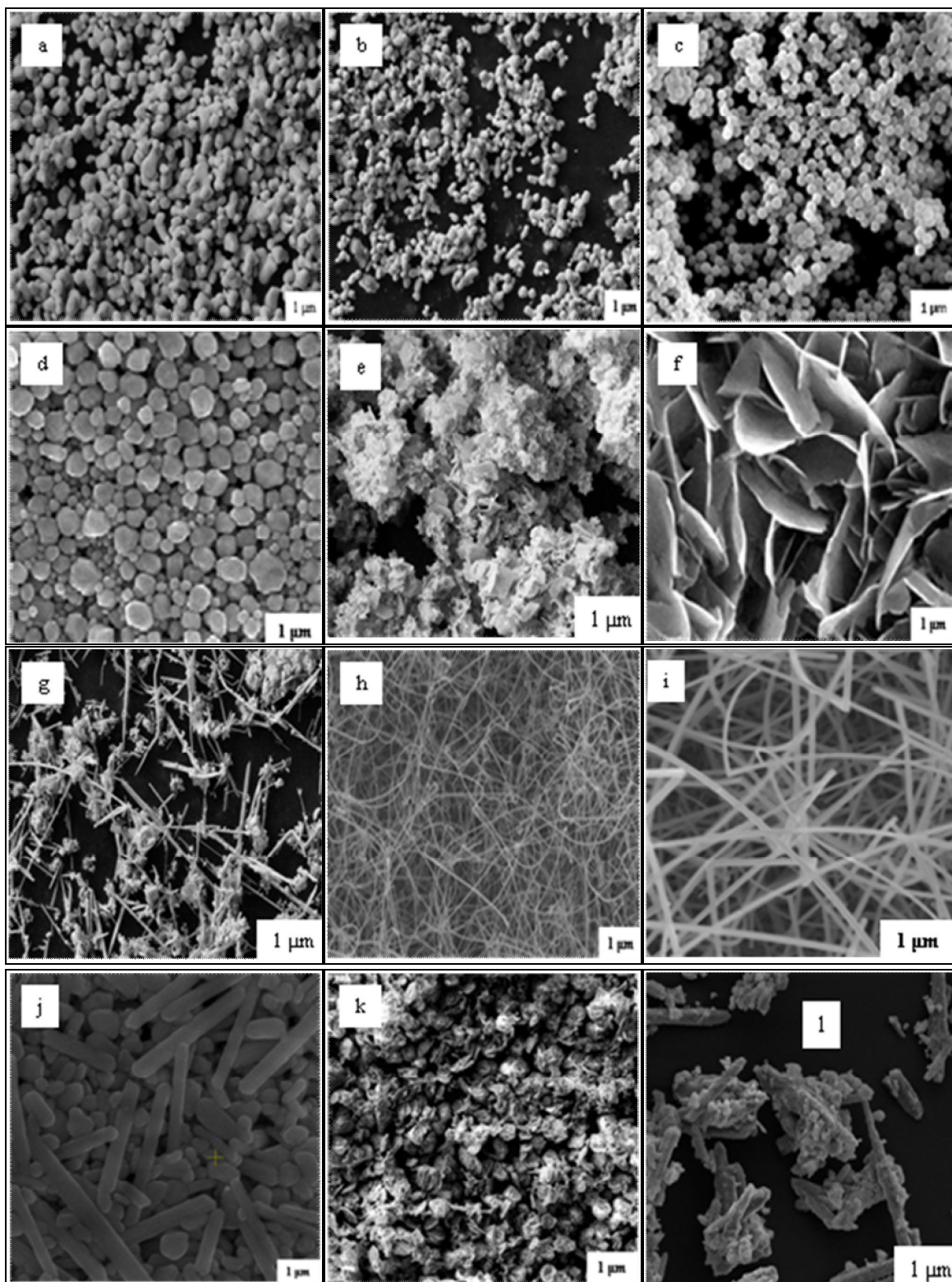
Figure 2: (a – l) Representative SEM images of various shaped Ag synthesis under salt mediated polyol process

Obviously, Ag nanowires must have been generated following self – seeding process previously explained [26, 27]. Relatively lower Ag^+ precursor concentration accounts for a reduced chemical potential which favours thermodynamically stable multiply twinned particles (MTPs) (table 1, fig. 2a,b). Maintaining that condition with Cl^- addition favours oxidative etching of the MTPs and the resultant overriding growth led to nanowires (fig. 2h). However, there was a significant change in length and diameter of the nanowires as the PVP/Ag^+ is reduced to 0.3 while keeping 50% salt addition. This led to increased growth rate of the etched MTPs leading to longer and thicker nanowires (Fig. 2i). A report elsewhere [23] indicated contributory effort of Fe^{2+} in promoting production of nanowires. Cu^{2+} has also aided reduction of $AgNO_3$ [24]. At PVP/Ag^+ ratio and 10% Zinc salt intervention a perfect nanosphere (table 1, fig. 2c) of diameter 48 nm resulted within 75 min. However, a cross – check experiment under the same condition and without salt mediation offered quazi nanosphere in 3 hours reaction time.
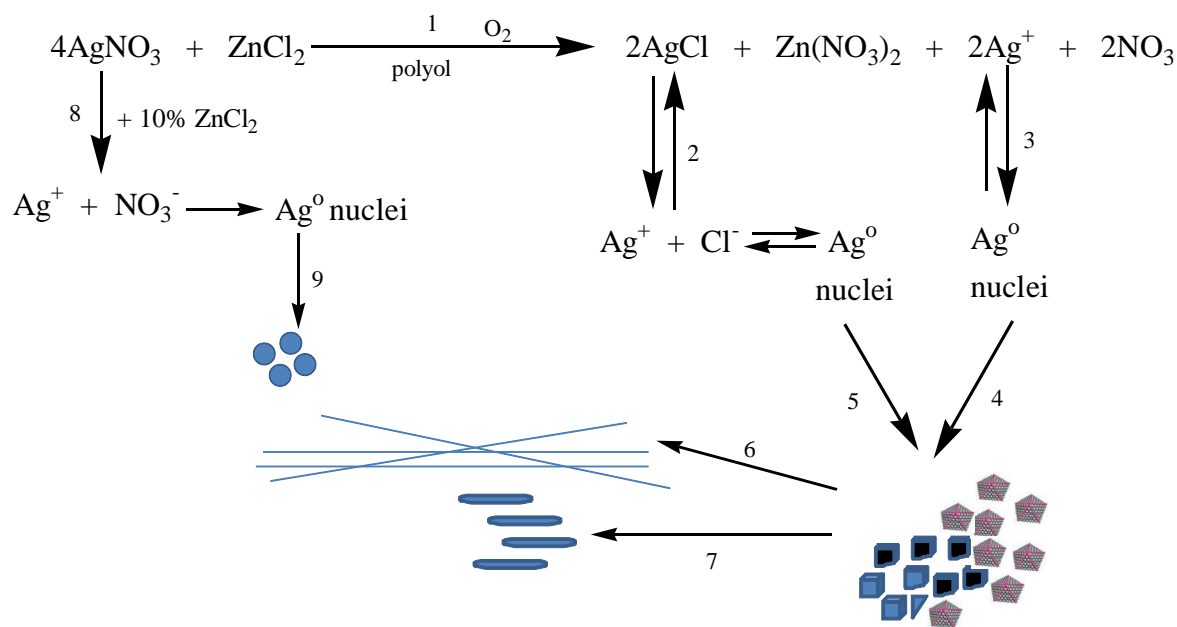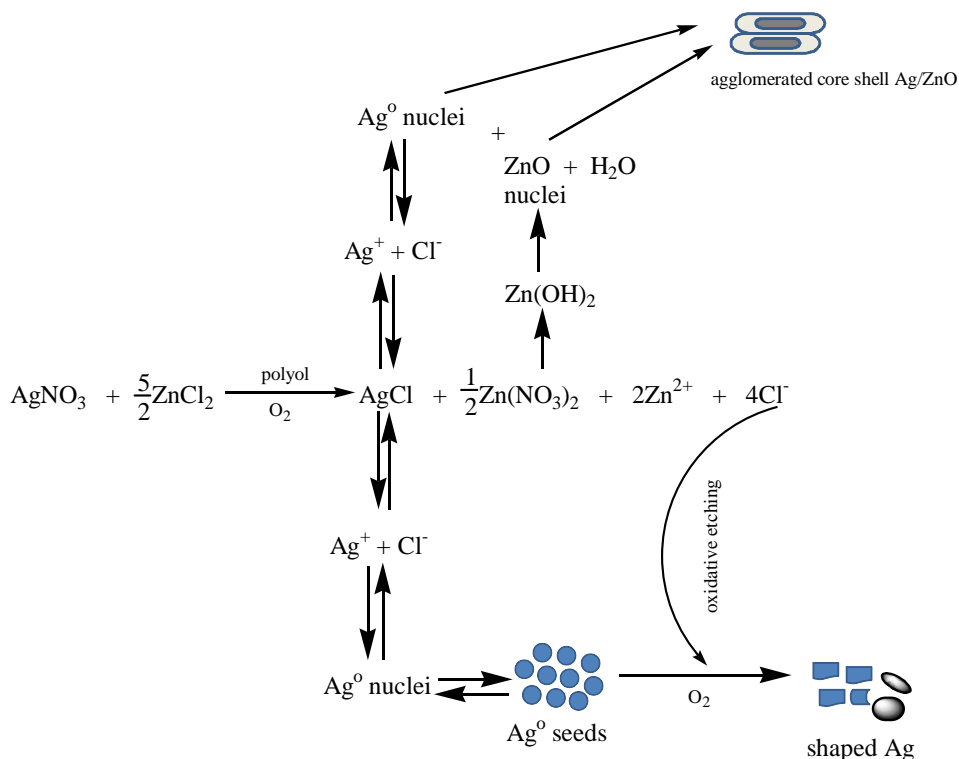

Scheme 1: Proposed synthetic pathway for some shaped Ag nanoparticles when low mole% of the salt was used.

Scheme 1 explained the formation of shaped Ag which however depends on the level of Cl^- mediation vis-à-vis the nature of polyol. Following path 8 and 9 of the scheme, Ag^+ are reduced to Ag^o, nucleation occurs and seed formation led to quazi nanosphere whose seed growth proceeded in an isotropic manner (OD particles). Since nanosphere belong to the lowest energy shape, simple reduction of the silver precursor is expected with or without exotic reagent. In this case, synergy effect of the salt has been noted towards formation of a perfect nanosphere within 75 min in hopefully

kinetically controlled manner. Hopefully, the synergy efforts of both Zn^{2+} and PVP lowered {100} surface energy and brought down reaction time to 75 min from 120 min spent without salt contribution.

PVP has been shown to preferentially adsorb onto the {100} surface of silver particles where it served to stabilize and protect the small single-crystal seeds [28]. Insufficient molar concentration of PVP to lower surface energy usually give room for the production of twin detects via a higher surface energy [25].

The morphology of the seed particles is one important parameter that decides anisotropic growth of noble metal nanoparticles; the process that supports what shape dominate is an index of twinning probability [29]. Following reaction sheme 1 shaped anisotropic growth Ag emanated from both AgCl and Ag^+ (path 2 and 3) due to large excess of $AgNO_3$ present in the solution. The only few Cl^- came from AgCl which dissolved as the temperature is increased beyond 150 ^oC. Ag^+ concentration in the medium is sufficient enough to promote twinning process amidst some oxidative etching effect of Cl^-/O_2 of the initially formed MTPs. Under this condition, the growth rate from decahedra to 1D anisotropic products is faster and which compete overwhelmingly with etching rate. In DEG, high Ag^+ concentration around the growing nuclei pushes in high twining probability requisite for MTPs formation from where nanorod and nanowires were grown.

Scheme 1: Proposed synthetic pathway for some shaped Ag nanoparticles when high mole% of the salt was used.

As the concentration of Ag^+ is reduced and Cl^- in the reaction medium significantly increased while keeping DEG as reducing solvent (Scheme 2), the morphologies of the Ag formed changed beyond scientific expectation and tuned towards 2D anisotropic nanostructures (nanoflakes and nanosheets) depending on the amount of Cl^- in the reaction medium as indicated in the table. The plausible explanation to this observation is that Ag^o atoms around the growing Ag nuclei are significantly low and that prevented twinning probability for MTPs. Therefore, The scenario displayed promoted extensively high Cl^-/O_2 oxidative etching which may lead to unequally grown {100} and {111} facets of silver. Eventually, Cl- supposedly suppress the crystal growth along the {111} direction [30]. Obviously, the area ratio of {100}/{111} facet varies depending on the relatively growth rate of the two surfaces, resulting in differences in particle shapes [30]. Therefore, the formation and structural changes observed for nanoflakes → nanosheets can be explain by the Cl^-/O_2 etching vis-à-vis site specific deposition of AgCl on the surface of Ag nanoparticle seeds [31]. In other words, selective adsorption of Cl^- on the {111} plane of Ag seeds and the formation of AgCl, also in contact with the seeds, plays roles in the nanosheets and nanoflakes formation as promoted by DEG.

Interestingly, reaction in the presence of GL while keeping equal ratio of PVP/Ag^+ offered what we may name as a fluffy round nanocake (fig. 2k). This observation further shows that the type of aldehyde emanated from the polyol, which in this case GL causing the reduction process is also important in the shape determination of the growing silver seeds. The predominating anisotropic 1D nanorod (78 nm diameter, 352 nm length on the average, fig. 2j) obtained is similar to that previously reported [32].

To further clarify if indeed Zn^{2+} Cl^- has significant effect on the morphological changes of the nanoparticles, one may ask after what happens when Cl^- is greatly increased. To answer this, mole% of $ZnCl_2$ was made up to 300 and reaction carried out under reflux condition. Representative SEM spectrum in figure 2l shows what we may call ZnO – wrapped Ag nanocomposite which obviously followed a core – shell model as monitored by UV – vis absorption spectroscopy (spectra not shown for brevity) and XRD.

The XRD pattern (fig. 1a) of the as – prepared Ag core–ZnO shell is quite revealing and distinct in terms of crystallinity and peaks attributable to the heterostructure (OD on 1D). This exceptional distinct nature of the crystalline phases peaks rules out the possibility for an alloy formation as there is no evidence of intimate association of ZnO within Ag matrix. The C_{Ag}/C_{ZnO} ratio in the core-shell is *ca* 6.4, indicating a large core enrichment of the Ag. Structural evolution of Ag–ZnO

(fig 1b) from Ag (fig. 1a) has been demonstrated with the emanation of peaks (1010), (0002), (1011), (1012), (1120) and (1013) which are due to ZnO nanostructure.

The plausible mechanism of formation of agglomerated Ag–ZnO can be followed from scheme 2. Obviously, Ag nanorod resulted from dissolving AgCl and $Zn(NO_3)_2$ offererd $Zn(OH)_2$ precipitate which was transformed into ZnO nuclei. The ZnO nuclei grew and self assembled itself on the Ag nanorod surface due to relative surface energy concepts.
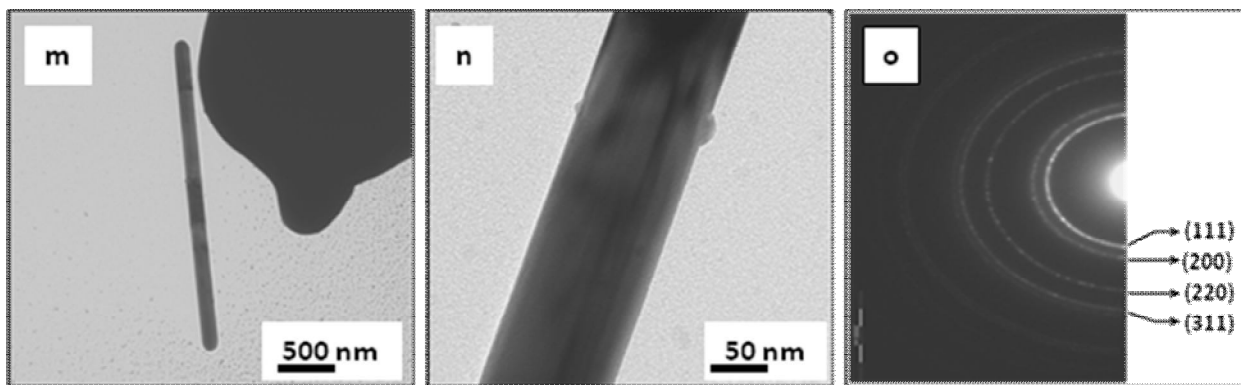

Figure 3: Representative TEM images of (m) Ag nanorod (n) Ag nanowire obtained at different level of salt mediation. (o) Electron diffraction pattern recorded from the Ag nanowire shown in image n

The morphologies and structures of some of the shaped silver nanoparticles were investigated by TEM, EDX and UV-Vis spectroscopy. Figures 3m and 3n are the representative TEM of the anisotropic 1D structures of nanorod and nanowire respectively, which are crystalline in nature. Electron diffraction pattern recorded from figure 3n displays characteristic rings which could be index as the (111), (200), (220) and (311) allowed refelections from fcc silver.
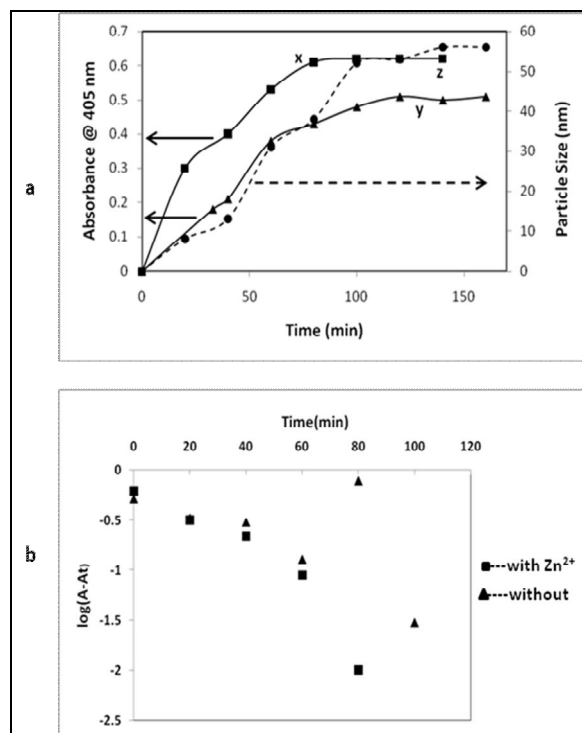
Figure 4: Growth Kinetic of the nanosphere formation with or without salt mediation (a) plots of absorbance and particle sizes against time (b) plot of log (A – At) against time.

Growth kinetic of the nanosphere seed formation was studied with the view to further clarifying the influence of Zn^{2+} Cl^- as it affects reaction rate. The absorption of silver at 405 nm and corresponding particle sizes are plotted against time (fig 4a). Curve z (dotted line ------) represents the particle sizes evolution as the nanosphere grew. Curve x and curve y are those with and without $ZnCl_2$ salt respectively. In both cases, absorbance and particle size increase with increasing time until when equilibrium was attained after which there was no further growth. However, absorbance of Ag nanosphere under the mediating influence of salt was significantly higher (curve x) indicating increased particle density. A plot of log(A – At) against time (fig. 4b) is quite revealing and conclusive the effect of salt mediation. Calculated rate constant ($k = 4.6$ x 10^{-1} S^{-1}) under salt influence has been found to be almost three times higher than that without salt mediation ($k = 1.6$ x 10^{-2} S^{-1}). Apparently, nucleation and growth process vis-à-vis particle size of the perfect nanosphere could be kinetically controlled to reach equilibrium and which eventually brought the reaction to completion within 75 min in contrast to that which was not mediated taking up to 120 min reaction time. Both cation and anion may be responsible for this observation [33]. Certainly, Zn^{2+} influenced the rate of reaction and size equilibrium while Cl^- is responsible for the shape of nanoparticles formation.
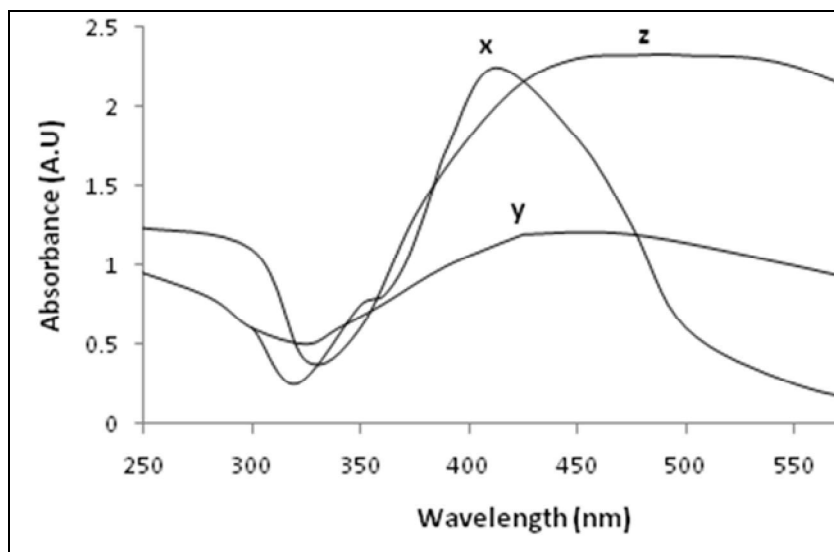
Figure 5: UV – vis Absorption spectrum of (x) nanosphere (y) nanorod and (z) nanowire

It has been established that copper, gold and silver display Plasmon absorption in the visible region. However, silver in particular usually have an absorption maximum at 404 nm [34].The UV-visible spectra of silver nanosphere , nanorod and nanowires synthesized are showed in Figure 5 with corresponding curves x, y and z respectively. Ag nanosphere which is of the lowest energy displays absorption maximum at 421 nm while Ag nanorod and Ag nanowire shows red – shifted plasma absorption maximum at 452 nm and 484 nm respectively. The reason behind the discrepancies in the observed optical properties is attributed to increase in aspect ratio as the morphologies change from spheres to rods and wires, the larger the aspect ratio the more red- shifted the longitudinal Plasmon band [35,36]. Moreover, the shifting experienced by the nanorod and nanowire are due to enhanced absorption of visible light along their respective length and width [36]. Nanowire is longer and is therefore more red – shifted.

It worth noting that accidentally acquired results obtained on the core – shell Ag/ZnO heterostructure, though agglomerated, seems hopeful if further experimental measures are taken. Study in this direction on full scale basis is underway.

In conclusion, it has been established that $ZnCl_2$ salt vis-à-vis variations in PVP/$AgNO_3$ ratio and type of polyol to a large extent have influence on the nucleation, growth and final shapes of silver nanostructure. The mole% of the salt relative to the silver precursor determined whether the Ag seed formation proceeded in an isotropic or anisotropic manner which in this case was found to depend on twinning probability, amount of Cl^- and Ag^+ in the reaction mixture. Ag shape formation was either initiated via seed growth arising from MTPs leading to nanowires and nanorods or via Cl^-/O_2

leading to other shapes (flakes, sheets, cake e.t.c) depending on the extent of etching and polyol used. Extremely high mole% of the salt has been found to be contributory factor to the development of Ag core–ZnO shell heterostructure bearing OD on 1D. In particular, the strategies to control the kinetic and formation of desired nuclei with twin planes during nucleation offered option for anisotropically shaped silver nanostructures. The type of polyols adopted has been found to be responsible for that option.

Acknowledgment

References

[1] C.M. Lieber, Bull MRS. 28 (2003) 486-49.

[2] M.P. Pileni Adv. Funct. Mater. 11 (2001) 323.

[3] S. Nie, S.R. Emory Science 275 (1997) 1102.

[4] P.V. Kamat, J Phys. Chem. B 106 (2002) 7729.

[5] Y. Sun, Y. Yin, B.T. Mayers, T. Herricks, Y. Xia, Chem. Mater 14 (2002) 4736.

[6] D. Zhang, J. Yang, J. Ma, H. Cheng, L. Huang, Chem. Mater, 16 (2004) 872.

[7] L. Suber, I. Sondi, E. Matijevic, D.V. Goia, J Colloidal Interface Sci. (2005) 288.

[8] D. Kim Jeong, J. Moon, Nanotechnology. 17 (2006) 4019.

[9] L.M. Liz-Marzan A.P. Philipse, J Phys. Chem. 99 (1995) 15120.

[10] M. Jin, X. Zhang, S. Nishimoto, Z. Liu, D.A. Tryk, T. Murakami, A. Fujishima Nanotechnology 18 (2007) 075605.

[11] A.R. Siekkinen, J.M. McLellan, J. Chen, Y. Xia, Chem. Phys. Lett 432 (2006) 491.

[12] J. Zhu, C. Kan, X. Zhu, M. J-G Wan, J. Han, Y. Zhao, B. Wang, G. Wang, Mater Res. 22 (2007) 1497.

[13] S. Chen, D.L. Carroll, Nano Lett 2 (2002) 1003.

[14] I. Callegari – Santos, D. Tonti, M. Chergui, Nano Lett. 3 (2003) 1565.

[15]S.H. Liou, S. Huang, E. Klimek, R.D. Kirby, Y.D. Yao, J. Appl. Phys. 85 (1999) 4334.

[16] I. Srnova – Sloufova, F. Lednicky, A. Gemperle, J. Gemperlova, Langmuir, (2000) 9928.

[17] M.P. Mallin, C.J. Murphy Nano Lett. 2 (2002) 1235.

[18] N. Sandhyarani, T. Pradeep, Chem. Mater. 12 (2002) 1755.

[19] D-H, Chen, C-J, Chen, J. Mater Chem. 12 (2002) 1557.

[20] N. Castillo, J.A. Tenorio-Lopez, M.J. Martinez Ortiz, L. Garcia, R. Perez, A. Conde, Acta Microscopia. 18 (2009) 287.

[21] P.B. Joshi, V.J. Rao, B.R. Rehani, A. Pratap, Indian J. Pure. Appl. Phys. 45 (2007) 9.

[22] M.S. Park, T-H Lim, T-M Jeon, J-G Kim, M.S. Gong. Macromol. Res. (2008) 308.

[23] B. Wiley Langmuir, 21 (2005) 8077.

[24] Y. Xia Adv. Mater. 15 (2003) 353.

[25]C.D. Sanguesa, R.H. Urbina, M. Figlarz, Solid State Chem. 100 (1992) 272.

[26] J. Mullin, Crystallization, Oxford University Press ISBN: 0750611294, New York, (1997).

[27] L.D. Marks, Experimental Studies of small Particles structures. Report on Progress in Physics. 57 (1994) 603 ISSN; 0034-4885.

[28] Y. Su, B. Mayers, T. Herrick, Y. Xia, Nano Lett. 3 (2003) 955.

[29] X.L. Tang, M. Tsuji, M. Nishio, P. Jiang, Bull. Chem. Soc. JP. 82 (2009) 1304.

[30] Z.L. Wang, T.S. Ahmad, M.A. El-Sayed, Surf. Sci. 380 (1997) 302.

[31] R.S. Panikkanvalappil, S.Theruvakkattil, K.S. Akshaya, P. Thalapil, Nano Rev. 2 (2011) 5883.

[32] E. Braun, Y. Eichen, U. Sivan, G. Ben-Joseph, Nature 391 (1998) 775.

[33] K.E. Korte, S.E. Skrabalak, Y. Xia, J. Mater. Chem. 18 (2008) 437.

[34] T. Itakura, K. Torigoe, K. Esumi, Langmuir. 11 (1995) 4129.

[35] M.A. El-Sayed, Acc. Chem. Res. 34 (2001) 257.

[36] S. Link, M.B. Mohamed, M.A. El-Sayed, J. Phys. Chem. B 103 (1999) 3073.